Guaranteed bounds on highway travel times using probe and fixed data

Christian G. CLAUDEL*, Aude HOFLEITNER†, Nicholas D. MIGNEREY‡ and Alexandre M. BAYEN§

November 9, 2008

88^{th} TRB Annual Meeting

Word count: 5175 words in text + 6 figures = 6675 words

*Ph.D. Student, Department of Electrical Engineering and Computer Sciences, University of California, Berkeley CA, 94720-1710. claudel@eecs.berkeley.edu. Corresponding Author.

†Visiting scholar, Systems Engineering, Department of Civil and Environmental Engineering, University of California, Berkeley CA, 94720-1710. Graduate student, Ecole Nationale des Ponts et Chaussees, 6 et 8 avenue Blaise-Pascal-Cite Descartes Champs-sur-Marne - 77455 Marne-la-Vallee cedex, France

‡Visiting scholar, Systems Engineering, Department of Civil and Environmental Engineering, University of California, Berkeley CA, 94720-1710. Student, Ecole Centrale de Paris, Grande Voie des Vignes 92295 Chatenay Malabry Cedex, France

§Assistant Professor, Systems Engineering, Department of Civil and Environmental Engineering, University of California, Berkeley, CA, 94720-1710.

Abstract

This article investigates the problem of incorporating mobile probe data collected from GPS equipped cell phones into estimation algorithms for travel time. We use kinematic wave theory to create a modeling framework capable of incorporating trajectory data into the model. The problem of including loop detector data in this model is performed using a standard approach available in the literature. The problem of fusing this data with probe data is formulated using the Moskowitz function, which results from kinematic wave theory. Using this formulation, two linear programs are posed to compute upper and lower bounds travel time through the corresponding section of highway. The method thus provides a guaranteed range for the average travel time experienced by vehicles on the highway. The method is illustrated with data collected during the *Mobile Century* experiment on February 8th, 2008, using 100 Nokia N95 phones traveling onboard cars driving loops on I880 in California. A sampling and penetration rate study shows that the method provides accurate travel time estimates for penetration rates as low as 0.1% and spatial sampling strategies on the order of 0.2 miles. The performance of the method is illustrated with several case studies, in which measurements gathered by a few vehicles are sufficient to significantly improve results obtained from sparse loop detectors.

1 Introduction

Global scale traffic monitoring. Over time, the demand for mobility has dramatically increased, leading to a $78 billion annual drain on the U.S. economy in the form of 4.2 billion lost hours in commute and 2.9 billion gallons of wasted fuel, which amounts to 58 fully-loaded supertankers [25]. While there is almost no space for additional roads or freeways in the vast majority of urban and suburban environments, there is an enormous potential gain from real-time knowledge of traffic. This information has the potential to enable system solutions such as *ramp metering* [36], *dynamic speed limits* [19] and individual level solutions in which drivers can access traffic in real-time, and obtain customized itineraries and schedules from their location to avoid major congestion. Currently, only major freeways are instrumented in the US. The fundamental missing piece of information is that of secondary itineraries including expressways and arterial roads. Current traffic information comes from fixed sensors, for example loop detectors in the pavement [21], RFID transponders, radars or cameras [20]. While this information can easily be accessed on the internet [42, 43, 44, 45] and on phones using cell phone versions of these websites, these services only provide information where the transportation network is equipped with such detectors. To provide a global solution to this traffic information gathering problem, one needs traffic information everywhere where there is congestion within the transportation network. Given the high costs of deploying a traffic monitoring system and the lack of public infrastructure, mobile probes provide a feasible alternative for this problem. With the notable exception of the data from dedicated fleets [26] such as the police force, taxis, FedEx, UPS (all of which have very limited coverage), such traffic data simply does not exist on a *global scale*.

Smartphones as traffic probe sensors. In this context, the convergence of communication and sensing on multi-media platforms such as smartphones provides the engineering community with unprecedented monitoring capabilities. Smartphones such as the Nokia N95 now include a video camera, numerous sensors (accelerometers, light sensors, GPS), communication outlets (wireless, radios, bluetooth, infrared, USB, jack video-output / microphone), computational power and memory. The rapid penetration of GPS in phones enabled geolocalization and context awareness, leading to the explosion of *Location Based Services* (heavily relying on mapping) using phones. Their low cost, portability and computational capabilities make smartphones useful for numerous sensing applications in which they act as sensors moving with humans embedded in the built infrastructure. Large scale applications include traffic flow estimation [40], physical activity monitoring for assisted living at home [29], geotagging [18], and population migration tracking [17, 2]. In this context, smartphones appear as a viable source of traffic data which can be used to complement existing traffic sensors.

Incorporation of probe data into traffic models. One of the major challenges in using mobile probe data for traffic estimation is the difficulty to incorporate this data into traffic models, which are traditionally used to describe highway traffic. Several types of models can be used: statistical models [22, 4], and flow models [24, 32]. When a flow model is used, this process is known as *inverse modeling* or *data assimilation*: it consists in incorporating data in the mathematical model of a physical system, in order to estimate the current state of the system and forecast its future state [23, 3]. In the field of inverse modeling, *Lagrangian* sensing specifically refers to measurements performed along a sensor's trajectory which it usually cannot control. Examples of this are smartphones traveling onboard cars following highway traffic flow. This is in contrast to *Eulerian* sensing, in which sensors are fixed (for example, video cameras or

loop detectors along highways) and monitor a specific control volume in a static manner. While inverse modeling using Lagrangian sensors is a well established field in oceanography [23, 3], it is still a relatively novel technique in the field of transportation engineering. Traditional approaches such as *Kalman Filtering* (KF) have been applied to traffic models to perform estimation, in particular using first order models such as the *Cell Transmission Model* (CTM) [10, 11], see in particular [27, 35, 34, 28]. *Extended Kalman* (EKF) filtering has been used to handle second order models, when the discretization scheme used allows it, see for example [37]. For more complicated problems involving partial differential equation models, *Ensemble Kalman Filtering* (EnKF) [15] has been used for speed estimation on the highway [38, 39]. All the aforementioned methods produce a best estimate of traffic (in some sense, for instance in the least square sense), sometimes with statistics related to the produced results, such as confidence or probability associated with the prediction.

Problem statement. The present work investigates a practical problem which goes beyond the specific problem data assimilation (i.e. production of an estimate):

Problem 1: Given a set of loop detectors, and given a set of probe vehicles equipped with GPS, (i) how to reconstruct travel time, (ii) how to produce a guaranteed range for travel time, given the knowledge of the data?

This problem specifically addresses needs from the traveling public, since it is aimed at providing the public with the travel time information [8], and a range of validity of this information. The term "guaranteed range" refers the possible range of travel times, taking into account the uncertainties in the model, and assuming that the loop detector and probe data are exact. In addition, we also investigate the following problem:

Problem 2: What is the influence of the penetration rate of equipped vehicles and of the spatial sampling strategy on the range of the travel time estimation?

This second problem is helpful for cellular network operators and cellular phones manufacturers, who are currently in the process of mapping the transportation network with "virtual detectors", i.e. GPS data collection mechanisms which partly rely on the geometry of the transportation network.

Organization of the article. This article is organized as follows: Section 2 summarizes the flow models used in this study. In Section 3, we describe a specific spatial strategy currently used by Nokia to sample traffic, and explain how this type of data can complement existing loop detector data. The section finally summarizes the data assimilation procedure used and the corresponding algorithm developed for the estimation of travel time and the corresponding range of interest. In section 4, the method is implemented using the *Mobile Century* data set [14, 38, 39], which consists of loop detector and GPS-based smartphone data collected for 8 hours of traffic on I880 in Union Landing, CA, for 100 vehicles equipped with Nokia N95 phones. This section presents some conclusions of numerical results obtained for travel time estimation, as well as a study of the influence of penetration rate and spatial sampling strategy.

2 Background

2.1 Traffic flow models

Kinematic wave theory. Traffic flow on a highway segment can be described using both density and flow functions, which represent an aggregated number of vehicles per space (respectively time) unit. The present article uses the *Lighthill-Whitham-Richards* (LWR) *partial differential equation* (PDE) [24, 32], which is a first order model obtained from conservation of vehicles and an empirical relation between vehicle flow $q(t,x)$ and vehicle density $\rho(t,x)$:

$$\frac{\partial \rho(t,x)}{\partial t} + \frac{\partial q(\rho(t,x))}{\partial x} \;=\; 0 \tag{1}$$

The flow-density relation $q(\rho)$ is known as *flux function* or *fundamental diagram* [33, 1, 6]. In the remainder of this article, we use a triangular diagram [10, 11, 13], as commonly done in the literature:

$$q(\rho) = \begin{cases} v\rho & \text{if} \quad \rho \in [0, \rho_c] \\ w(\rho_c - \rho) + v\rho_c & \text{if} \quad \rho \in [\rho_c, \rho_{\max}] \end{cases}$$

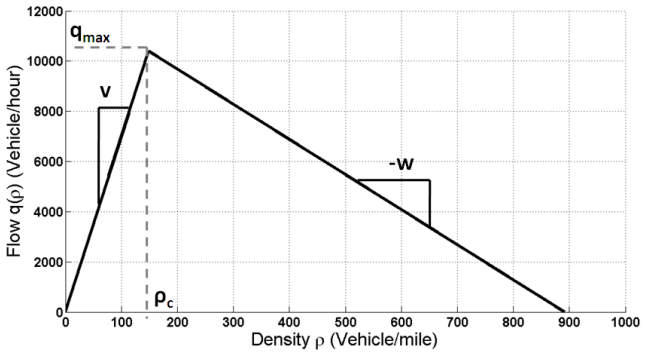

Figure 2.1: Representation of a triangular flux function.

In the previous diagram, v is the free flow speed, ρ_c is the critical density, and $\rho_{\max}$ is the maximal density. All these quantities are illustrated in Figure 2.1. The capacity of the road is the maximal flow $q_{\max} = \rho_c\, v$. The parameters v, w, ρ_c and $\rho_{\max}$ are related by $\rho_{\max} w = \rho_c(v + w)$, which means that the triangular fundamental diagram is fully characterized by three parameters.

Because density is an aggregated quantity, which cannot be measured by probe vehicles directly, the LWR PDE is difficult to use as such to incorporate vehicle trajectory data available from probe vehicles. Instead, we use an alternate (equivalent) representation of traffic which was introduced by Newell and Daganzo, following the work of Moskowitz [30, 12, 13]. The *Moskowitz function* $\mathbf{M}(t,x)$ uses consecutive integer labels assigned to vehicles entering the highway at a user defined location $x = x_{\text{in}}$, counted from the reference point $(t = 0, x = x_{\text{in}})$, where the first vehicle is assumed to label 0. Assuming that vehicles do not pass each other, one could imagine that an observer at location $x = x_{\text{in}}$ numbered the vehicles as

they passed him. The Moskowitz function $\mathbf{M}(t,x)$ (also known as *cumulative number of vehicles function*) represents the number of the last vehicle to pass an observer at location x before time t, and encodes the distribution of the vehicles on the highway at all times. The space and time derivatives of the Moskowitz function are related to the flow and density functions as follows [31, 12, 13]:

$$\frac{\partial \mathbf{M}(t,x)}{\partial t} = q(\rho(t,x)) \qquad \text{and} \qquad \frac{\partial \mathbf{M}(t,x)}{\partial x} = -\rho(t,x). \tag{2}$$

Using equation (2), one can transform equation (1) into the following Moskowitz *Hamilton-Jacobi* PDE [12, 13]:

$$\frac{\partial \mathbf{M}(t,x)}{\partial t} - q\left(-\frac{\partial \mathbf{M}(t,x)}{\partial x}\right) = 0. \tag{3}$$

Solution of the Moskowitz HJ PDE. Solutions to PDE (3) are known [9, 16] and can be computed with standard numerical analysis tools. Solving equation (3) requires the knowledge of the initial state of the highway, i.e. the knowledge of an initial function $\mathbf{M}_0(x) := \mathbf{M}(0,x)$ at time $t = 0$, which would represent a distribution of labels of vehicles initially on the highway. Note that when this knowledge is not available, one can use the "flush" effect of the highway (i.e. waiting long enough until initial vehicles have disappeared from the section of interest) to avoid the need for this data. Assuming that loop detector data is available at locations $x = x_{\text{in}}$ (upstream) and $x = x_{\text{out}} > x_{\text{in}}$ (downstream), one can prescribe counts at these locations, i.e. $\mathbf{M}(t, x_{\text{in}}) = \gamma(t)$ and $\mathbf{M}(t, x_{\text{out}}) = \beta(t)$, where $\gamma(t)$ and $\beta(t)$ are the vehicle counts measured by the detectors. In other words, the label $\gamma(t)$ is incremented by one each time a car drives by the location $x = x_{\text{in}}$. A similar rule applies at $x = x_{\text{out}}$. Finally, given a vehicle with an integer label $\overline{\mathbf{M}}_i$ and a trajectory given by $x_i(t)$, we know that the value of the function $\mathbf{M}(t, x_i(t))$ is constant and equal to $\overline{\mathbf{M}}_i$, because along the trajectory $x_i(t)$ of vehicle $\overline{\mathbf{M}}_i$, the value of the label $\overline{\mathbf{M}}_i$ does not change, thus $\mathbf{M}(t, x_i(t)) = \overline{\mathbf{M}}_i$ for all times t during which the vehicle is on the corresponding segment of highway. The corresponding *initial*, *boundary* and *internal* conditions on the function $\mathbf{M}(t,x)$ can thus be summarized by:

- Initial condition $\mathbf{M}(0,x) = \mathbf{M}_0(x)$ — Vehicle distribution at initial time
- Left boundary condition $\mathbf{M}(t, x_{\text{in}}) = \gamma(t)$ — Inflow of vehicles
- Right boundary condition $\mathbf{M}(t, x_{\text{out}}) = \beta(t)$ — Outflow of vehicles
- Internal conditions $\overline{\mathbf{M}}(t, x_i(t)) = \mathbf{M}_i$ — Trajectory measurement for the vehicle labeled $\overline{\mathbf{M}}_i$ for all i

2.2 Reconstruction of a posteriori travel time function

This work is focused on the computation of the *a posteriori* travel time $TT(t)$ at time t using the knowledge of the Moskowitz function. The *a posteriori* travel time is defined as follows. If a vehicle $\overline{\mathbf{M}}_i$ crosses the upstream boundary x_{in} of the highway at time τ, and crosses the downstream boundary x_{out} at time t, the a posteriori travel time $TT(t)$ is defined by $TT(t) = t - \tau$, and represents the time necessary to cross the road section observed by the vehicle $\overline{\mathbf{M}}_i$ leaving the highway at time t. The a posteriori travel time can thus be obtained from the boundary condition functions $\gamma(\tau)$ and $\beta(\tau)$ using the following procedure:

Algorithm 1 *Algorithm for computing the travel time function*

1.	*Input* t	*(time at which one wants to compute travel time)*
2.	*Read* $\overline{\mathbf{M}} := \beta(t)$	*from downstream loop detector*
3.	*Find* τ *such that* $\gamma(\tau) = \overline{\mathbf{M}}$	*from upstream loop detector (using backtracking search)*
4.	*Compute* $TT(t) := t - \tau$	*(if* τ *exists)*

3 Data assimilation using mixed Eulerian/Lagrangian Data

3.1 Model of label evolution and trajectories

Boundary conditions. Figure 3.1(a) illustrates the physical interpretation of the boundary conditions $\gamma(\cdot)$ and $\beta(\cdot)$ of the Moskowitz function in terms of the loop detector counts. As can be seen in this figure, data is prescribed at $x = x_{\text{in}}$: $\mathbf{M}(t, x_{\text{in}}) = \gamma(t)$ where $\gamma(t)$ is the label function at x_{in}, which is constructed from the loop detector measurements by summing the vehicles as they pass it. For example, if the label of the vehicle passing at $t = 17$ (min) is $\gamma(17) = 25$, and five vehicles pass between $t = 17$ (min) and $t = 18$ (min), then $\gamma(18) = 22$. Similarly, downstream, at $x = x_{\text{out}}$: $\mathbf{M}(t, x_{\text{out}}) = \beta(t)$ where $\beta(t)$ is the label function at x_{out}, which is constructed from the loop detector at $x = x_{\text{out}}$.

Initial conditions. The knowledge of the initial vehicle distribution (similar to an aerial picture of the road at time $t = 0$), would give the initial condition represented with a dash line, in other words the labels of cars as initially positioned on the highway. The corresponding function is called $\mathbf{M}_0(x)$. For example, if we (arbitrarily) label the vehicle at $x = x_{\text{in}}$ and $t = 0$ vehicle zero ($\mathbf{M}(0, x_{\text{in}}) = 0$), and if there are 20 vehicles between $x = x_{\text{in}}$ and $x > x_{\text{in}}$, then $\mathbf{M}(0, x) = -20$. Note that the labels can all be arbitrary shifted by the same amount, which is prescribed at x_{in}: if one arbitrarily decided to call the vehicle at $x = x_{\text{in}}$ vehicle 28, i.e. $\mathbf{M}(0, x_{\text{in}}) = 28$, we would have $\mathbf{M}(0, x) = 8$. It can easily be seen that this shift does not matter in equation (3) as long as it is the same for all x and t, since the PDE only depends on derivatives of $\mathbf{M}(\cdot, \cdot)$. For practical reasons, initial condition data is not easily measurable. The method proposed next does thus not assume knowledge of $\mathbf{M}_0$.

Probe vehicle conditions. In Figure 3.1(a) the solid trajectory line on the time-space diagram represents the successive locations where the phone can be probed along a vehicle trajectory. For privacy reasons, the system does not track entire trajectories of the vehicles (it is represented this way on the figure for illustration purposes – in practice only subsets of this trajectory would be transmitted to the system). For these subsets of trajectories, we know that at time t when a measurement comes (the vehicle being at position $x = x_i(t)$), the label function $\mathbf{M}(t, x_i(t))$ at this location and time will be equal to the label $\overline{\mathbf{M}}_i$, i.e. $\mathbf{M}(t, x_i(t)) = \overline{\mathbf{M}}_i$.

3.2 Computation of the boundary condition functions using loop detector data

Figure 3.1(b) illustrates the procedure used in this article to collect data used for the data assimilation procedure.

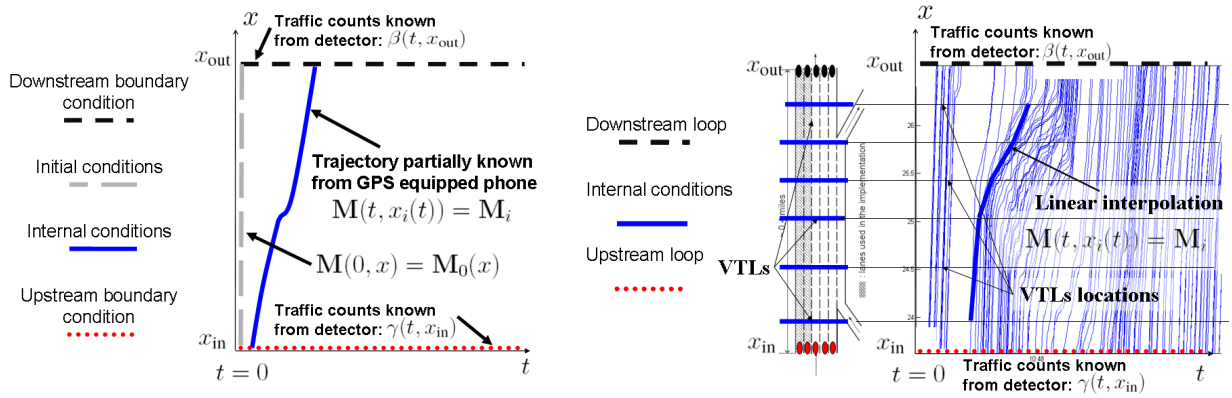

(a) Illustration of the notation used in the kinematic wave theory.

(b) Data collection procedure used by the algorithm. The data used for the picture comes from the *Mobile Century* experiment [41].

Figure 3.1: Physical interpretation of the boundary conditions on the Moskowitz function.

Assimilation of the boundary conditions. The data assimilation procedure developed in this article requires us to incorporate loop detector data (flow data only) into the flow model. For this, the knowledge of the functions γ and β is necessary. By definition of these loop detector flows, γ and β can be obtained (modulo a constant) by direct integration of the flows measured by the detectors. Thus, calling $q_{\text{inflow}}(t)$ the flow measured by the upstream detector and $q_{\text{outflow}}(t)$ the flow measured by the downstream detector, we have:

$$\gamma(t) = \int_0^t q_{\text{inflow}}(\theta)d\theta \qquad \text{and} \qquad \beta(t) = \int_0^t q_{\text{outflow}}(\theta)d\theta + \Delta \tag{4}$$

The parameter Δ represents the value[1] of $\beta(0, x_{\text{out}})$. The total number of vehicles present on the highway at time $t = 0$ is $-\Delta \geq 0$, which is an unknown of our problem. If the parameter Δ was known (for instance by taking a picture of the highway at initial time and counting the total number of vehicles on the highway), then the a posteriori travel time could be computed exactly, assuming that the loop detector flow data was errorless. However, since it is not the case, the parameter Δ must be estimated. Algorithm 1 can then be used to compute the travel time. As will appear in the next sections of this algorithm, Δ is never known a priori (unless $\mathbf{M}_0$ is known, which is difficult in practice). It will therefore become one of the decision (dummy) variables of the algorithm.

Assimilation of the probe data. Internal conditions of the problem are collected using a system called *Virtual Trip lines* (VTLs). VTLs are geographical markers stored in the client (i.e. the mobile handset), which trigger a position and speed update whenever a probe vehicle crosses them. A VTL can thus be viewed as a virtual loop detector, which can collect speed information for vehicles crossing it. These VTLs are part of a Nokia proprietary system which ensures the privacy of the users. In essence, it provides readings of the $x_i(t)$ function at specific geographical locations on the highway according to a sampling procedure

[1] Note that $\gamma(0) = 0$ by assumption.

used by Nokia to guarantee privacy of the users. Figure 3.1(b) shows how this data becomes available to us. As can be seen from Figure 3.1(b) probe data is known at sampling locations (VTLs), between which vehicle trajectories are assumed to be linear.

3.3 Linear Program formulation of the data assimilation problem

Integration of the loop and probe data into the model. The problem of integrating initial, boundary and internal conditions into the Moskowitz equation (3) is in general extremely challenging. In this article, we decompose this complex problem into many simple problems associated to each of the value conditions (initial, boundary, and internal). For this, we define a *component* function associated to each value condition that must be satisfied by the Moskowitz function [6, 7] as follows:

- *Initial condition component:* $\mathbf{M}_{\mathbf{M}_0}(t,x)$. This initial condition function can be computed directly from the initial condition $\mathbf{M}_0(x)$; it encodes the dependence of the solution on the initial condition.
- *Left boundary condition component:* $\mathbf{M}_\gamma(t,x)$. This left boundary condition function can be computed directly from the left boundary condition $\gamma(t)$; it encodes the dependence of the solution on the left boundary condition (upstream loop detectors).
- *Right boundary condition component:* $\mathbf{M}_\beta(t,x)$. This right boundary condition function can be computed directly from the right boundary condition $\beta(t)$; it encodes the dependance of the solution on the right boundary condition (downstream loop detectors).
- *Internal condition component:* $\mathbf{M}_{\overline{\mathbf{M}}_i}(t,x)$. This internal condition function can be computed directly from the trajectory $x_i(t)$ of vehicle $\overline{\mathbf{M}}_i$; it encodes the dependance of the solution on the internal condition.

The component functions can be computed individually using dynamic programming methods [12, 13], a Lax-Hopf formula [1], or using the minimization of closed-form expression functions [7]. When physical compatibility conditions are met [6], the solution to the Moskowitz equation (3) can be simply computed as the minimum of the component functions [1, 6, 7]:

$$\mathbf{M}(t,x) = \min\left(\mathbf{M}_{\mathbf{M}_0}(t,x), \mathbf{M}_\gamma(t,x), \mathbf{M}_\beta(t,x), \mathbf{M}_{\overline{\mathbf{M}}_1}(t,x), \ldots, \mathbf{M}_{\overline{\mathbf{M}}_n}(t,x)\right) \tag{5}$$

In order to be able to simultaneously impose the initial, boundary and internal conditions, these conditions must satisfy necessary and sufficient conditions known as *compatibility conditions* [6, 7]. Indeed, in arbitrary initial, boundary and internal conditions cannot be simultaneously imposed on the Moskowitz function. For instance, if the initial condition consists in a completely congested highway, no positive inflow can be imposed at the entrance x_{in}, since there is no available space for entering vehicles. Similarly, if the highway is initially empty, no positive outflow can be imposed since no cars are present.

Linear program formulation. We define the decision variable X as $X := (\Delta, \overline{\mathbf{M}}_i, \overline{\mathbf{M}}_2, \ldots, \overline{\mathbf{M}}_n)$ where n is the total number of probe vehicles used for the internal conditions. The compatibility conditions can be shown to be equivalent to a set of k linear inequalities[2] in the variable X. The mathematical proof

[2]The number k depends upon the type of conditions used for the reconstruction, the repartition of the car trajectories, and the time horizon.

of this fact is cumbersome and algebraically involved. It is out of the scope of this article [5]. The linear inequalities resulting from [5] can be written formally as $AX \leq b$, where $A \in \mathbb{R}^{k \times n+1}$ and $b \in \mathbb{R}^k$. The matrix A and the vector b depend upon the inflow, outflow, and trajectory data.

We define the vector c as $c^T = (1, 0, 0, \ldots, 0)$. Using this definition, we can express Δ as $\Delta = c^T X$. Since we are interested in the value of Δ only, we consider the following *Linear Programs* (LPs):

$$\begin{array}{lll} \textbf{min:} & c^T X & \qquad \textbf{max:} \quad c^T X \\ \textbf{s.t.:} & AX \leq b & \qquad \textbf{s.t.:} \quad AX \leq b \end{array} \tag{6}$$

The solution of the above LPs yield two objective values $\Delta_{\min}$ and $\Delta_{\max}$, which can be interpreted as follows: the value $-\Delta_{\min}$ represents the maximal number of vehicles that can possibly be present on the highway, and the value $-\Delta_{\max}$ represents the minimal number of vehicles that must be present on the highway (assuming our data is exact). Since $\Delta \in [\Delta_{\min}, \Delta_{\max}]$, we can compute a corresponding range of travel times $TT_{\min}(t)$ and $TT_{\max}(t)$ using Algorithm 1. The overall method is represented in Algorithm 2.

Algorithm 2 *Process used to construct travel time ranges from Eulerian/Lagrangian measurements.*

1. *Input* *Loop detector data (flow data) and VTL data*
2. *Compute* *Boundary and internal conditions* γ, β *and* μ_i
3. *Compute* A *and* b
4. *Compute* $\Delta_{\min}$ *and* $\Delta_{\max}$ *(using LP (6))*
5. *Compute* $TT(t)$

4 *Mobile Century* Implementation

In this section we implement the previous procedure using loop detector data, probe vehicle data, and video detector data collected during a field experiment known as *Mobile Century*. We present an analysis of the sampling strategies and the number of equipped vehicles to implement this algorithm in practice.

4.1 Description of the experiment

The *Mobile Century* [41] experiment took place on February 8th, 2008. It was conducted on Highway I-880, near Union City, CA, between Winton Ave. and Stevenson Blvd. (see Figure 4.1). This 10-mile long section of highway was selected specifically for its complex traffic properties, which include alternating periods of free-flowing, uncongested traffic, and slower moving traffic during periods of heavy congestion. The section also has a high density of loop-detectors (17 loops on the section of interest). The data from these sensors is collected by the *Freeway Performance Measurement System* (PeMS).

The experiment consisted in deploying 100 GPS- equipped Nokia N95 cell phones on a freeway during eight hours. 165 UC Berkeley students drove loops on the section of interest between 10am and 6pm. This period encompasses both free flow and congested traffic, and the transition between the two of them.

The data was collected in two ways during the experiment.

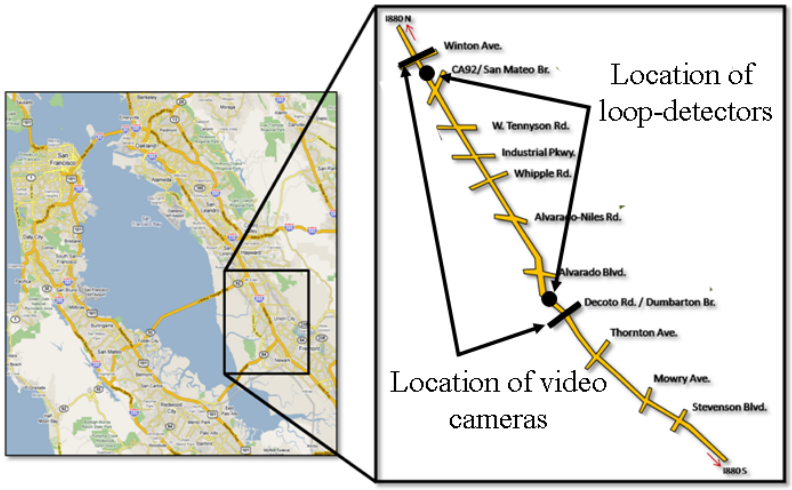

Figure 4.1: Set-up of the *Mobile Century* experiment. The figure represents the placement of the video camera and the loop detectors selected for the computation and the validation of our results.

(i) A privacy preserving architecture was developed, which uses the concept of *Virtual Trip Line* (VTL) explained earlier. During the experiment, we deployed 40 VTLs in the section of interest (each VTL covers both travel directions). This data was used to produce real-time travel time and speed estimates on the section of interest and presented to the press in real-time [41]. The method used a data assimilation algorithm based on *Ensemble Kalman Filtering* (EnKF) [38], which provided an estimate of travel time. On February 8^{th}, 2008, the goal of the algorithm was to show the possibility of reconstructing speeds and travel time in real-time from a set of probe vehicle measurements.

(ii) Each cell phone was storing its position and velocity every three seconds. This data (trajectory data) was stored for archival purposes in order to evaluate the quality of the data a posteriori. It was only generated for experimental validation, and would not be collected in an operational system.

In order to validate the estimation results of all algorithms developed during this project, video data was collected from three bridges in the deployment area. The travel times were experimentally measured using a set of six HDV cameras running on the Mowry Ave., Decoto Rd. and Winton Ave. overpasses. The video data was sent to six laptops which were synchronized before the experiment and archived the data with timestamps. The camera footage was analyzed after the experiment, and the identifiable license plates (approximately 70% of the vehicles) were subsequently stored in a database. A matching algorithm was used to compute travel time through license plate reidentification. Figure 4.1 shows the deployment area of two of the three camera locations used to produce the data presented in this article. In the rest of the article, the corresponding travel time data will be depicted by dots in the figures of the subsequent sections.

4.2 Analysis of probe vehicle penetration and VTL spacing

This section presents an analysis of probe vehicle penetration rate and VTL spacing, using the data presented in the previous section.

Penetration rate. The penetration rate achieved during the experiment was 3% to 5% depending on the time of the day [14]. We use VTL data collected at each of the 40 VTL deployed on the section of highway. In an operational system, not all VTL measurements would be used by the system to probe all the vehicles systematically. In practice, a vehicle traveling across a VTL is randomly probed. For the present study, we assume that all vehicles are sampled, and we artificially decrease the number of measurements used by the algorithm in order to simulate lower penetration rates. This procedure is a way to degrade the data set in order to assess the performance of the algorithm for low penetration rates.

VTL degradation. In order to study the influence of VTL spacing on the quality of the results, we also reduce the available VTLs deployed for this study, i.e. artificially suppress some of them in our parametric study. The goal of this procedure is to study the performance of the algorithm when measurements are spatially sparse.

Parametric study of penetration rate and VTL sampling. Using the two decimation procedures outlined above, we solve the two linear programs (6) for $\Delta_{\min}$ and $\Delta_{\max}$ for each of the penetration rates and the VTL spacing chosen in the study. For each of these values, the length of the period considered for the assimilation is one hour and 25 minutes. The corresponding bounds on travel times (computed from the $\Delta_{\min}$ and $\Delta_{\max}$) are obtained for a vehicle initially entering the segment of interest. The results are summarized in Figure 4.4. In this figure, we plot for each pair (penetration rate - VTL spacing) the difference $TT_{\max}(t) - TT_{\min}(t)$. This range represents the guaranteed bound on average travel time (subject to the overtaking assumption and perfect data assumption). As expected, the range is the smallest for high penetration rates and low VTL spacing. The best corresponding range provided by the method is of the order of 100 seconds, for an average travel time of about 1200 seconds. This corresponds to a 8% error provided by the method. These results are very encouraging: they show that even with low penetration rates, and reasonable VTL spacing, the method is able to evaluate a guaranteed range for average travel time within less than 10% of its actual value. This type of information is very helpful for deployment studies, in order to determine the operational conditions for which this system would become valuable.

4.3 Results

Figures 4.3 and 4.4 illustrate the numerical results obtained by solving problem (6).

- Figure 4.2 shows the range of travel times provided by the method if loop detectors only are used. Obviously, with two loop detectors separated by 6.06 miles, the range cannot be tight because of the extremely large uncertainty of traffic when only two measurement stations are available for such a long distance. As can be seen in this figure, the cloud of validation data (obtained from video) is included in this range. The figure also shows the estimate which would be obtained by reading the PeMS speed data directly (which falls outside of the range and is far from the validation data). As can be seen in the right subfigure, the estimate using all 16 PeMS speed detectors existing in this section falls inside the range and is closer to

the could of points (at the expense of using 16 detectors instead of 2 as in the previous figure).

- Figure 4.3 represents the guaranteed bounds on the travel time obtained from the algorithm throughout the experiment duration. As expected, this range gets tighter as the number of vehicles increases. The addition of a single vehicle trajectory already produces drastic improvements in the predicted range. By construction of the optimization program, incorporating new trajectory information adds new constraints, which can only reduce the size of the feasible set $AX \leq b$, thus reducing $\Delta_{\max} - \Delta_{\min}$ and the range of guaranteed average travel times. Since the non-overtaking assumption is clearly wrong, and since the data is inexact, the ranges computed for the travel time function do not necessarily encompass exactly the actual travel times anymore. The next section provides explanations for this fact. Note however that, while there might be some relatively small error with these bounds, one can clearly see from these four figures that the estimates are not only tight, but also reproduce the large scale trends of the data (in the present case the progressive decrease of travel time as morning congestion dies out).

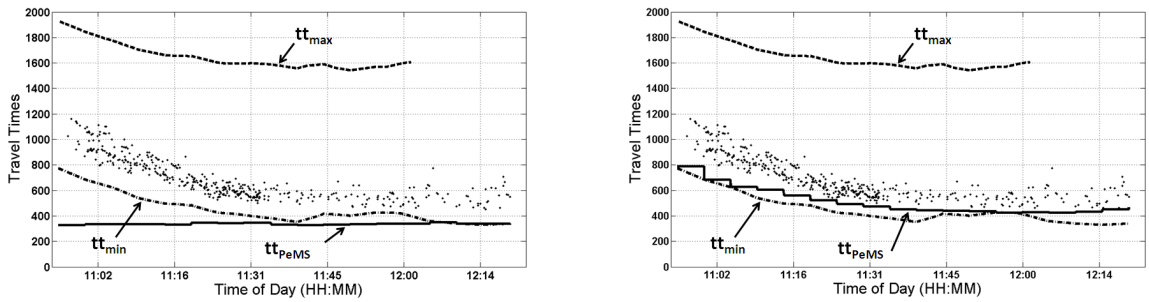

Figure 4.2: Comparison of the computation of the travel time using our algorithm and a naive method based on integration of the speed data given by the loop detectors. Loop detector data only is used in this example (no VTL data). The horizontal axis represents the time t (unit: hours and minutes). The vertical axis represents the travel time (unit: sec). The upper and lower bounds on travel time, computed by the algorithm (using flow data) described before, are represented by dashed lines. The actual travel times obtained from the video data are represented by dots. The travel time computed by the commonly used PeMS algorithm using velocity data is represented by a solid line. It uses only the first and last loop in the left figure, whereas all the intermediate loop are used in the right figure.

4.4 Comments on the results

The quality and validity of the results depends on the assumptions formulated for the model (in particular if they are satisfied experimentally) and the data. Measurements errors can have serious consequences on the accuracy of the method. We now analyze some of the sources of inaccuracy of the results.

- The model assumes that cars do not overtake each other (no shearing) and computes an associated possible range of travel times for all the vehicles driving at the same time. This is a common assumption in numerous transportation engineering articles. However, vehicles overtake each other, their label is not constant along their trajectory. As the distribution of the travel times (in Figure 4.3) do not

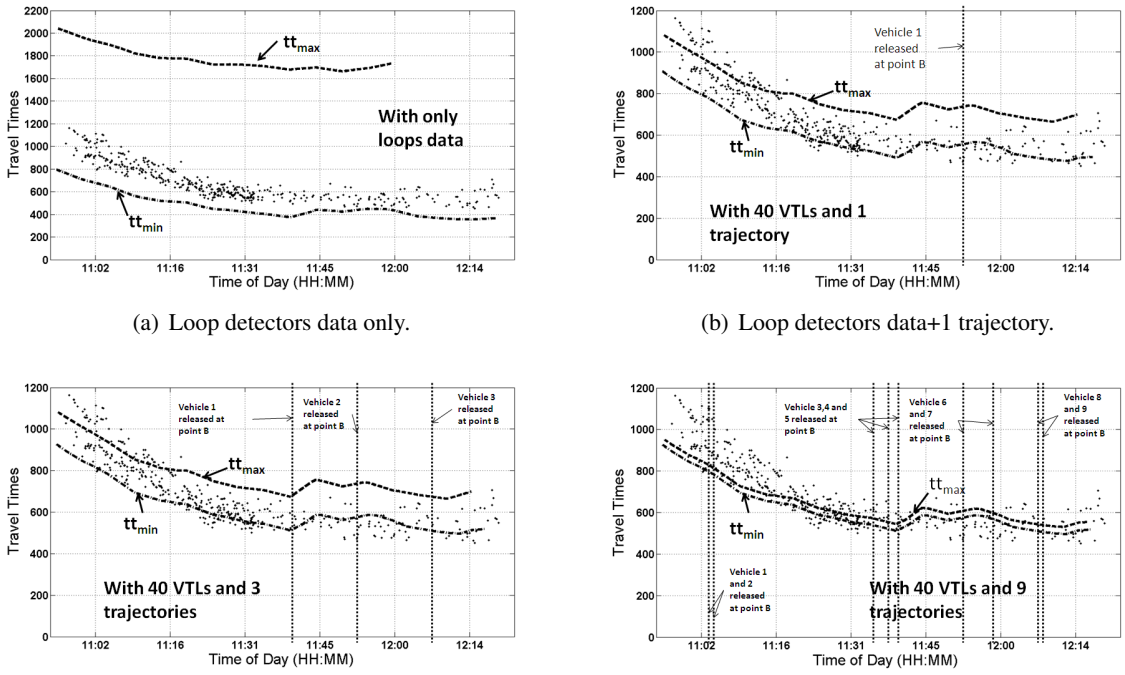

(a) Loop detectors data only.

(b) Loop detectors data+1 trajectory.

(c) Loop detectors data+3 trajectories.

(d) Loop detectors data+9 trajectories.

Figure 4.3: Estimation of the travel time function. The horizontal axes represent the time t (unit: hours and minutes). The vertical axes represent the travel time TT. Subfigure legends are the same as in the previous figure. The influence of the penetration rate (respectively 0%, 0.01%, 0.03% and 0.1%) is illustrated in the subfigures (respectively (a), (b), (c) and (d)).

satisfy the non-shearing assumption, some travel times may not satisfy the guaranteed bounds (which are computed for a non-shearing situation only).

- On and off ramps are not taken into consideration by this study, because of the lack of available data. The conservation of vehicles assumption is therefore violated. Data shows that the cumulative number of vehicles that exits the road section by the loop at point B is increasing faster than the cumulative number of vehicles that enter at point A. Over the course of eight hours, the difference reaches 9247 vehicles, which exceeds the road section capacity (5041 vehicles) and consequently invalidate this assumption. The model integrates this additional flow of vehicles as a constant throughout the day. But in the reality, this flow may vary with the time of day. The additional knowledge of inflows and outflows would improve the accuracy of the computation.

- Loop detector data is known to be noisy and biased. Loop detectors report their raw data to the PeMS system every 30 seconds. This raw data is hardly directly useable. PeMS filters this data and averages it on a five minutes time period. Despite the filtering and the data processing, this data still has significant issues which need to be addressed. The bounds are guaranteed only when the VTL and loop detector data are exact. Since this is never the case in practice, the guarantee is lost.

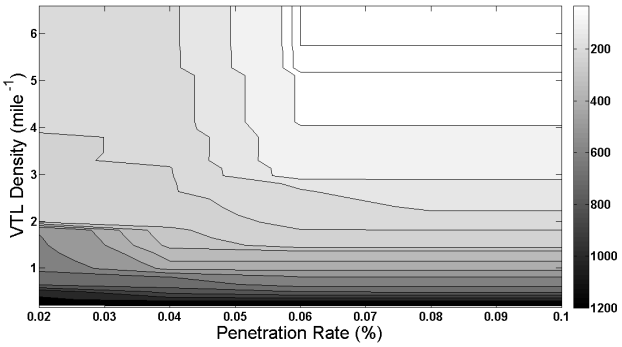

Figure 4.4: Guaranteed range (unit: seconds) for the estimation of the travel time $TT(t)$ for a randomly chosen time t. The horizontal axis represents the penetration rate (unit: percent) of the GPS-equipped phones in the traffic. The vertical axis represents VTL density (unit: number of VTL per mile). The total error $TT_{\max}(t) - TT_{\min}(t)$ on the parameter $TT(t)$ is indicated using a grey scale, a darker shade representing a larger error.

- The time sampling of the loop detectors is low. The average five minute update gives a low time resolution for the boundary conditions. Using a confidence interval for the upstream and downstream boundary conditions increases the numbers of parameters to be estimated by the computation and improves the robustness of the model.
- Experimental set-up. The locations of the loop-detectors form the boundary of the road section considered for the computation of the travel time (this is illustrated in Figure 4.1). As these locations do not fit perfectly with the location of the video cameras (located on the bridges) giving the travel time used for the validation of the results, we interpolate the computed travel time on the section delimited by the cameras. As the road section considered for the computations (delimited by the loop detectors) represents 88% of the road section delimited by the cameras, we assume that the computed travel time is 88% of the travel time between the two video cameras. This is obviously an approximation, and induces additional numerical error.

5 Conclusion

This article investigates a specific data assimilation technique used to incorporate probe vehicle data into flow models. The study uses a traditional traffic flow model (the Lighthill-Whitham-Richards theory), formalized using the Moskowitz framework. This framework enables the use of a function, whose isolines correspond to vehicle trajectories. The problem of including loop detector data (flow data) in this framework is done following the traditional kinematic wave approach. The problem of fusing it with probe data is formulated using the Moskowitz function. Based on this formulation, two linear programs are created to compute upper and lower bounds of the estimate of initial numbers of vehicles on the highway segment. These bounds are taking into account the uncertainty in the model, and are used to find bounds on travel

time through the corresponding section of highway. The method is implemented on data collected during the *Mobile Century* experiment, using 100 Nokia N95 phones traveling onboard cars driving loops on I880 in California. A sampling and penetration rate study shows that the method provides accurate travel time estimates at low penetration rates and reasonable sampling strategies. The performance of the method is illustrated with several case studies in which travel time estimates using loop detector data only can be improved. We also show that the data gathered by a few vehicles is sufficient to significantly improve results obtained by sparse loop detectors. Future works will be dedicated to the estimation of travel times, taking into account the uncertainty of the data (in addition to the model uncertainty), and relaxing the non-overtaking hypothesis.

ACKNOWLEDGMENTS

The authors are grateful to Jean Pierre Aubin, who developed the mathematical framework used in this article, for his vision, his guidance and his scientific generosity. We thank Patrick Saint-Pierre for his help on setting the first version of the code used for this study and for fruitful conversation. The algorithms developed in this article are using technology produced by the company VIMADES. The authors also wish to thank Saurabh Amin and Dan Work for their help and valuable suggestions.

References

[1] J.-P. AUBIN, A. M. BAYEN, and P. SAINT-PIERRE. Dirichlet problems for some Hamilton-Jacobi equations with inequality constraints. *In press: SIAM Journal on Control and Optimization*, 2008.

[2] H. BAR-GERA. Evaluation of a cellular phone-based system for measurements of traffic speeds and travel times: A case study from Israel. *Transportation Research Part C*, 15(6):380–391, 2007.

[3] A. F. BENNETT. *Inverse Methods in Physical Oceanography*. Cambridge University Press, Cambridge, UK, 1992.

[4] P. BICKEL, C. CHEN, J. KWON, J. RICE, E. VAN ZWET, and P. VARAIYA. Measuring Traffic. *Statistical Science*, 22(4):581–597, 2007.

[5] C. G. CLAUDEL and A. M. BAYEN. Guaranteed bounds for traffic flow parameters estimation using mixed Lagrangian-Eulerian sensing. In *Proceedings of the 46th Annual Allerton Conference on Communication, Control, and Computing*, Allerton, IL, Sep. 2008.

[6] C. G. CLAUDEL and A. M. BAYEN. Lax-Hopf based incorporation of internal boundary conditions into Hamilton-Jacobi equation. Part I: theory. *Submitted to IEEE Transactions on Automatic Control*, 2008.

[7] C. G. CLAUDEL and A. M. BAYEN. Lax-Hopf based incorporation of internal boundary conditions into Hamilton-Jacobi equation. Part II: Computational methods. *Submitted to IEEE Transactions on Automatic Control*, 2008.

[8] B. COIFMAN. Estimating travel times and vehicle trajectories on freeways using dual loop detectors. *Transportation Research Part A*, 36(4):351–364, 2002.

[9] M. G. CRANDALL, L. C. EVANS, and P.-L. LIONS. Some properties of viscosity solutions of Hamilton-Jacobi equations. *Transactions of the American Mathematical Society*, 282(2):487–502, 1984.

[10] C. F. DAGANZO. The cell transmission model: a dynamic representation of highway traffic consistent with the hydrodynamic theory. *Transportation Research*, 28B(4):269–287, 1994.

[11] C. F. DAGANZO. The cell transmission model, part II: network traffic. *Transportation Research*, 29B(2):79–93, 1995.

[12] C. F. DAGANZO. A variational formulation of kinematic waves: basic theory and complex boundary conditions. *Transporation Research B*, 39B(2):187–196, 2005.

[13] C. F. DAGANZO. On the variational theory of traffic flow: well-posedness, duality and applications. *Networks and heterogeneous media*, 1:601–619, 2006.

[14] S. AMIN et al. Mobile century-using GPS mobile phones as traffic sensors: a field experiment. In 15^{th} *World congress on ITS*, New York, N.Y., November 16-20 2008. Intelligent Transport Systems.

[15] G. EVENSEN. *Data Assimilation: The Ensemble Kalman Filter*. Springer-Verlag, Berlin Heidelberg, 2007.

[16] H. FRANKOWSKA. Lower semicontinuous solutions of Hamilton-Jacobi-Bellman equations. *SIAM Journal of Control and Optimization*, 31(1):257–272, 1993.

[17] M. C. GONZALEZ, C. A. HIDALGO, and A.-L. BARABASI. Understanding individual human mobility patterns. *Nature*, 453:779–782, 2008.

[18] K. GREENE. A faster, more energy-efficient GPS: New software could help make location-aware devices ubiquitous. *MIT Technology Review (online)*, `http://www.technologyreview.com/Infotech/20781/?a=f`, May 16th, 2008.

[19] A. HEGYI, B. DE SCHUTTER, and J. HELLENDOORN. Optimal coordination of variable speed limits to suppress shock waves. *IEEE Transactions on Intelligent Transportation Systems*, 6(1):102–112, March 2005.

[20] J.-C. HERRERA and A. M. BAYEN. Traffic flow reconstruction using mobile sensors and loop detector data. In 87^{th} *TRB Annual Meeting*, Washington D.C., Jan. 12-17 2008. Transportation Research Board.

[21] Z. JIA, C. CHEN, B. COIFMAN, and P. VARAIYA. The PeMS algorithms for accurate, real time estimates of *g*-factors and speeds from single loop detectors. In *IEEE Intelligent Transportation Systems Conference Proceedings*, pages 536–541, Oakland, CA, Aug. 2001.

[22] A. KRAUSE, E. HORVITZ, A. KANSAL, and F. ZHAO. Toward community sensing. In *IPSN 2008, International Conference on Information Processing in Sensor Networks*, St. Louis, MI, Apr. 2008.

[23] J. M. LEWIS, S. LAKSHMIVARAHAN, and S. DHALL. *Dynamic Data Assimilation: A Least Squares Approach*. Cambridge University Press, Cambridge, UK, 2006.

[24] M. J. LIGHTHILL and G. B. WHITHAM. On kinematic waves. II. A theory of traffic flow on long crowded roads. *Proceedings of the Royal Society of London*, 229(1178):317–345, 1956.

[25] T. LOMAX and D. SCHRANK. Annual study shows traffic congestion worsening in cities large and small. Press Release, *Texas Transportation Institute*, College Station, TX, Sep. 2007.

[26] J. E. MOORE, S. CHO, A. BASU, and D. B. MEZGER. Use of Los Angeles freeway service patrol vehicles as probe vehicles. California Partners for Advanced Transit and Highways (PATH). Research Report: UCB-ITS-PRR-2001-05. Technical report, Feb. 2005.

[27] L. MUNOZ, X. SUN, R. HOROWITZ, and L. ALVAREZ. Traffic density estimation with the cell transmission model. In *Proceedings of the 2003 American Control Conference*, pages 3750–3755, Denver, CO, June 2003.

[28] L. MUNOZ, X. SUN, R. HOROWITZ, and L. ALVAREZ. A piecewise-linearized cell transmission model and parameter calibration methodology. In *Proceedings of the Transportation Research Board (TRB)* 85^{th} *Annual Meeting*, Washington D.C., Jan. 22-26 2006.

[29] B. NAJAFI, K. AMINIAN, A. PARASCHIV-IONESCU, F. LOEW, C. BULA, and Ph. ROBERT. Ambulatory system for human motion analysis using a kinematic sensor: Monitoring of daily physical activity in elderly. *IEEE transactions on Biomedical Engineering*, 50(6):711–723, 2003.

[30] G. F. NEWELL. A simplified theory of kinematic waves in highway traffic, part I: general theory. *Transporation Research B*, 27B(4):281–287, 1993.

[31] G. F. NEWELL. A simplified theory of kinematic waves in highway traffic, Part (I), (II) and (III). *Transporation Research B*, 27B(4):281–313, 1993.

[32] P. I. RICHARDS. Shock waves on the highway. *Operations Research*, 4(1):42–51, 1956.

[33] I. S. STRUB and A. M. BAYEN. Weak formulation of boundary conditions for scalar conservation laws. *International Journal of Robust and Nonlinear Control*, 16:733–748, 2006.

[34] X. SUN and R. HOROWITZ. Localized switching ramp-metering control with queue length estimation and regulation and microscopic simulation results. In *Proceedings of the* 16^{th} *IFAC World Congress*, Prague, Czech Republic, July 4-8 2005.

[35] X. SUN, L. MUNOZ, and R. HOROWITZ. Highway traffic state estimation using improved mixture Kalman filters for effective ramp metering control. In *Proceedings of the* 42^{nd} *IEEE Conference on Decision and Control*, pages 6333–6338, Maui, HI, Dec. 2003.

[36] X. SUN, L. MUNOZ, and R. HOROWITZ. Methodological calibration of the cell transmission model. In *American Control Conference*, Boston, MA, June 2004.

[37] Y. WANG and M. PAPAGEORGIOU. Real-time freeway traffic state estimation based on extended Kalman filter: a general approach. *Transportation Research Part B*, 39(2):141–167, 2005.

[38] D. WORK, O.-P. TOSSAVAINEN, S. BLANDIN, A. M. BAYEN, T. IWUCHUKWU, and K. TRACTON. An ensemble Kalman filtering approach to highway traffic estimation using GPS enabled mobile devices. To appear in *IEEE Conference on Decision and Control*, 2008.

[39] D. WORK, O.-P. TOSSAVAINEN, Q. JACOBSON, and A. M. BAYEN. Distributed sensing with mobile devices for traffic estimation on transportation networks. Submitted to *Allerton Conference on Communication, Control, and Computing*, 2008.

[40] D. B. WORK, A. M. BAYEN, and Q. JACOBSON. Automotive cyber-physical systems in the context of human mobility. In *National Workshop on High-Confidence Automotive Cyber-Physical Systems*, Troy, MI, April 2008.

[41] `http://traffic.berkeley.edu/`.

[42] `http://www.511.org/`.

[43] `http://maps.google.com/`.

[44] `http://www.inrix.com/`.

[45] `http://www.traffic.com/`.